Journal of Natural Resources and Environmental Management
http://dx.doi.org/10.29244/jpsl.15.6.1034

RESEARCH ARTICLE

OPEN ACCESS

Check for updates

Spatio-Temporal Detection of Vegetation Change and Recovery in Fire-Affected Peatlands of Sumatra, Indonesia

Yudi Setiawan[a,f], Kustiyo[b], Sahid Agustian Hudjimartsu[c], Marshela Aida Handayani[a], Awaludin Jamil[e], Erianto Indra Putra[d]

[a] Department of Forest Resource Conservation and Ecotourism, Faculty of Forestry and Environment, IPB University, IPB Dramaga Campus, Bogor, 16680, Indonesia
[b] Research Center for Geoinformatics, Research Organization for Electronics and Informatics, National Research and Innovation Agency (BRIN), Bandung 40135, Indonesia
[c] Study Program of Information Technology, Faculty of Science and Engineering, Ibn Khaldun University, Bogor 16129, Indonesia
[d] Department of Silviculture, Faculty of Forestry and Environment, IPB University, IPB Dramaga Campus, Bogor, 16680, Indonesia
[e] Study Program of Natural Resources and Environmental Management, Graduate School, IPB University, IPB Baranangsiang Campus, Bogor, 16129, Indonesia
[f] Center for Environmental Research, International Research Institute for Environment and Climate Change, IPB University, Bogor, 16680, Indonesia

Article History
Received 15 June 2025
Revised 2 August 2025
Accepted 15 October 2025

Keywords
Post-fire succession, Burn severity, EVI, NBR

ABSTRACT

Tropical peatlands are among the most fire-prone ecosystems in Southeast Asia, where recurrent burning causes long-term degradation, carbon loss, and biodiversity decline. Assessing spatio-temporal patterns of recovery is therefore essential for guiding effective peatland restoration and fire prevention strategies. This study investigated vegetation recovery dynamics in a fire-affected peatland in Sumatra, Indonesia. Multi-temporal satellite imagery was processed to extract the Enhanced Vegetation Index (EVI) and Normalized Burn Ratio (NBR). Fire frequency and severity were further analyzed through hotspot distributions and fire history. The results revealed that NBR and dNBR were highly effective in detecting burned areas and assessing severity, while EVI provided complementary perspectives on recovery trajectories. Vegetation in once-burned areas showed relatively steady regrowth, with EVI values approaching pre-fire levels after several years. In contrast, repeatedly burned areas exhibited slower and more heterogeneous recovery, with fluctuating EVI pattern reflecting vegetation growth succession. Field vegetation surveys confirmed that repeated fires drastically simplified forest structure, reducing tree and pole density and favoring shrubs and ferns such as *Stenochlaena palustris* and *Melastoma malabathricum*. Overall, the study demonstrates that fire frequency and severity are critical determinants of peatland recovery. The EVI offers valuable insights into vegetation dynamics, while NBR provides reliable fire history mapping. These findings underscore the importance of combining spectral indicators with ground-based vegetation data for long-term monitoring and highlight the need for targeted restoration strategies, including hydrological rewetting and assisted natural regeneration, in repeatedly burned peatlands.

Introduction

Tropical peatlands in Southeast Asia represent globally significant ecosystems due to their high carbon storage capacity, rich biodiversity, and important hydrological functions. However, these ecosystems are also highly vulnerable to anthropogenic disturbances and recurrent fires. Indonesia, in particular, has experienced frequent and severe peatland fires during El Niño years, when prolonged droughts dramatically increase fuel dryness and ignition potential. The catastrophic fires of 1997 and 2015 are two of the most prominent

Corresponding Author: Yudi Setiawan setiawan.yudi@apps.ipb.ac.id Department of Forest Resource Conservation and Ecotourism, Faculty of Forestry and Environment, IPB University, Bogor, Indonesia.

examples, resulting in widespread ecological degradation, severe transboundary haze pollution, and substantial economic losses [1,2].

Indonesian peat swamp forests are highly susceptible to fires due to their thick organic soil and high carbon content. When these areas are drained and degraded, they become highly flammable and can burn for extended periods, ranging from weeks to months. The construction of canals and the removal of vegetation further facilitate the ignition and spread of fires, especially during prolonged dry seasons associated with El Niño [3,4].

Sumatra island is among the region most severely affected by peatland fires. Numerous areas within this island, including those designated for restoration, have experienced recurrent fires due to historical land alterations, drainage systems, and persistent droughts. Repeated fires hinder vegetation regrowth, alter forest development, and have long-term impacts on forest structure and biodiversity [5,6]. The severity and frequency of fires are critical factors influencing post-fire vegetation recovery, with more severe or frequent fires typically resulting in slower recovery and greater ecosystem damage [7,8].

Understanding the long-term impacts of recurrent fires is crucial for planning restoration and fire prevention strategies in degraded peatlands. Satellite-based remote sensing is a valuable tool for studying these effects, as it enables the identification of burned areas, assessment of fire severity, and monitoring of vegetation regrowth over extensive areas and prolonged periods [9]. The Normalized Burn Ratio (NBR) is among the most widely used spectral indices for fire detection, taking advantage of the distinct spectral responses of vegetation and burned surfaces in the near-infrared (NIR) and shortwave-infrared (SWIR) regions. This index enables efficient identification of burned areas and supports assessments of burn severity by detecting reductions in vegetation moisture and structural integrity [10,11].

Following fire events, monitoring vegetation regrowth is essential to evaluate ecosystem recovery and resilience. In this context, the Enhanced Vegetation Index (EVI) has gained prominence as a robust tool for assessing vegetation dynamics, particularly in areas with high biomass or where atmospheric and soil background effects may interfere with traditional indices [12]. EVI incorporates a correction for aerosol scattering and soil influences, making it more reliable than the Normalized Differential Vegetation Index (NDVI) in densely vegetated or disturbed landscapes [13]. Its sensitivity to canopy structural variations allows for more accurate tracking of post-fire vegetation recovery, especially during the early and intermediate stages of regrowth [14]. By integrating NBR for initial fire detection and EVI for monitoring regrowth trajectories, remote sensing offers a powerful means to assess fire impacts and guide adaptive management in fire-prone tropical ecosystems.

By analyzing satellite images over time, researchers can discern patterns and variations in how landscapes recover post-fire, which assists in formulating evidence-based restoration plans [15–17]. This study concentrates on examining the recovery patterns of vegetation in a tropical peatland restoration area in Sumatra, Indonesia, that has been impacted by fire. Through multi-temporal spectral analysis, the research aims to elucidate the recovery trajectories following fires and contribute to the development of improved strategies for peatland restoration and fire management.

Materials and Methods

Study Area

This research was carried out in tropical peatland ecosystems across several sites in Sumatra that have experienced significant degradation due to recurrent fires and anthropogenic disturbances (Figure 1). Detailed field observations were conducted in multiple peatland restoration areas and fire-affected peatland landscapes to capture the variability of post-fire vegetation recovery. One of the focal study sites is the Merang-Kepayang region of South Sumatra Province, Indonesia, encompassing approximately 22,280 hectares. This area is characterized by degraded peat swamp forests, which have undergone significant ecological alterations due to prolonged anthropogenic disturbances. The site has a documented history of repeated fires, often exacerbated by prolonged dry seasons and El Niño climatic conditions. The earliest recorded fire considered in this study occurred in 1997, a period when the area was under active forest exploitation permits. Additional fire events were recorded in 2000 and 2004, coinciding with a period of ambiguous land tenure and minimal institutional oversight. Since 2008, the area was briefly managed under a peatland restoration initiative, although fire activity was still observed in 2010. The cumulative impacts

culminated in severe fire outbreaks during the extreme drought period between November 2014 and July 2015, underscoring the critical need for long-term monitoring and restoration interventions.

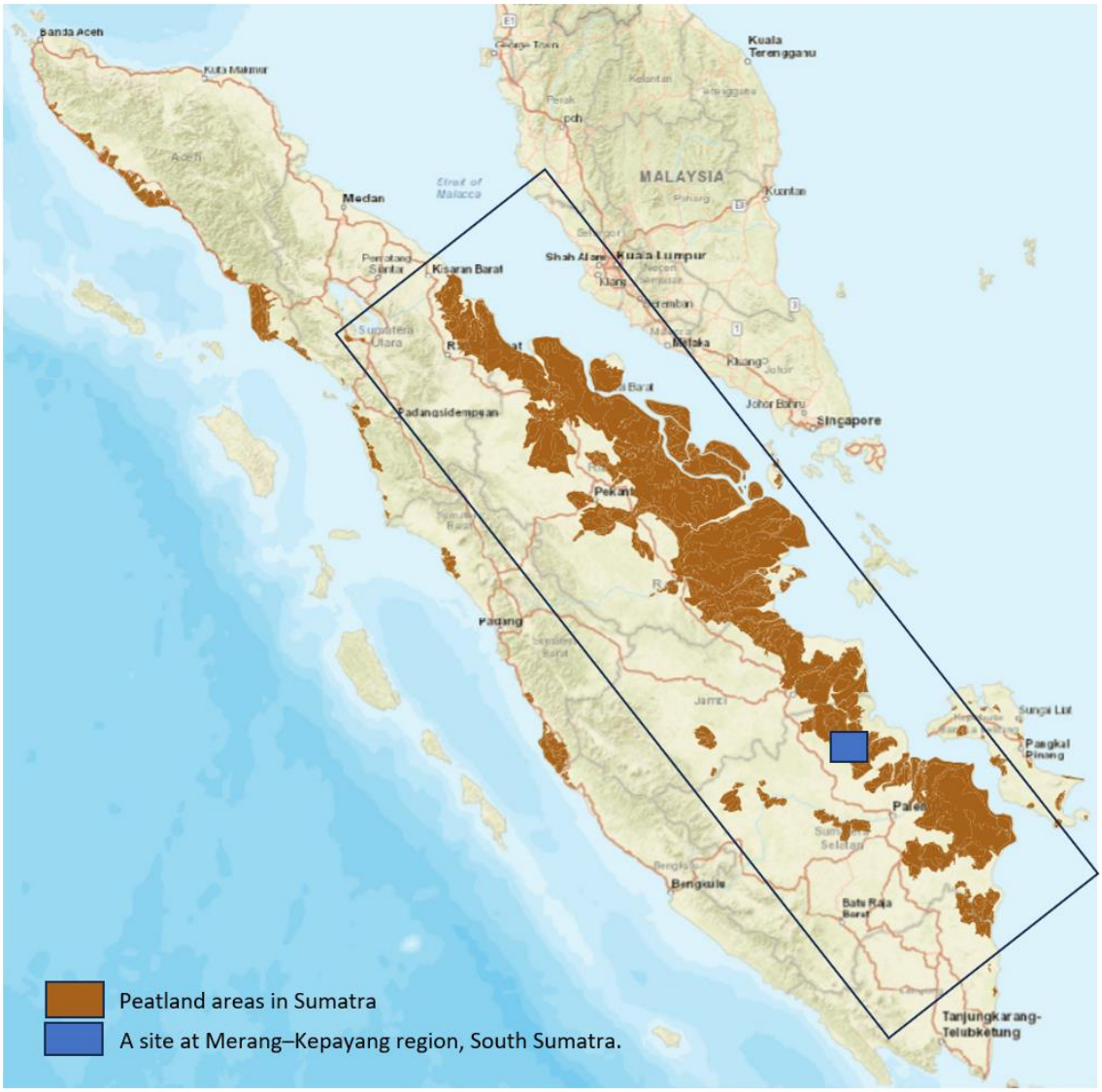

Figure 1. Study area: peatland ecosystems along the eastern coast of Sumatra, Indonesia.

Satellite Data

This study utilized multi-sensor satellite data to capture vegetation dynamics in tropical peatland ecosystems of Sumatra. The primary dataset was the Moderate Resolution Imaging Spectroradiometer (MODIS) Surface Reflectance product (MOD09A1), which provides consistent temporal coverage for large-scale monitoring. A set of Hierarchical Data Format (HDF) tiles covering the island was selected to ensure complete spatial representation of the study area. The datasets were obtained from NASA's Land Processes Distributed Active Archive Center (LP DAAC) and the USGS Earth Resources Observation and Science (EROS) Center (https://e4ftl01.cr.usgs.gov/MODIS/). To support pre-processing, auxiliary datasets such as water-masking layers and a 5° × 5° tiling system were also employed.

The MOD09A1 product provides estimates of land surface reflectance from MODIS sensors aboard the Terra satellite. It includes seven spectral bands, of which four were primarily used in this study: Red, Blue, Near-Infrared/NIR, and Shortwave Infrared/SWIR. MOD09A1 is available as an 8-day composite at a spatial resolution of 500 m, representing the best possible pixel observations during each compositing period based on minimal cloud contamination, low aerosol content, and favorable viewing geometry [18]. These data were employed to compute vegetation indices such as the Enhanced Vegetation Index (EVI), which combines Red, NIR, and Blue bands to enhance sensitivity to vegetation structure while reducing atmospheric and soil

background effects. The NIR band is sensitive to vegetation biomass and leaf area index (LAI), the Blue band aids in atmospheric correction, and the SWIR band provides information on vegetation water content and stress.

To complement the moderate resolution analysis provided by MODIS, Landsat Surface Reflectance products (30 m spatial resolution) from Landsat 7 ETM+ and Landsat 8 OLI/TIRS were incorporated for detailed assessments in selected peatland restoration sites. The inclusion of Landsat data addresses the limitation of MODIS spatial resolution, which constrains the detection of fine-scale land cover dynamics. This limitation is particularly evident in several regions, where transient land cover dynamics may occur at scales smaller than the minimum detectable extent, or where complex land cover mosaics can influence threshold-based change detection [19]. By leveraging Landsat's higher spatial detail, the analysis was able to capture localized disturbances, regrowth trajectories, and heterogeneity in vegetation recovery within restoration blocks.

Hotspot Data Processing

This study employed historical hotspot data spanning the period 1997 to 2021 as a proxy for fire occurrences. The digital hotspot records were obtained from NASA's MODIS sensors aboard the Terra and Aqua satellites, as well as from the Visible Infrared Imaging Radiometer Suite (VIIRS), filtered using a confidence level greater than 80% [20]. The dataset was analyzed in both temporal and spatial dimensions: temporal patterns were examined to identify peak fire periods, while spatial analyses were conducted to determine the location and distribution of hotspot clusters.

Spectral Indices for Vegetation Monitoring and Fire Impact Assessment

This study makes use of two spectral indices, namely the Enhanced Vegetation Index (EVI) and the Normalized Burn Ratio (NBR). Of these, EVI serves as the primary index for analyzing temporal dynamics of vegetation patterns, owing to its enhanced sensitivity in high-biomass regions and its capacity to reduce atmospheric and soil background effects [12]. The EVI is computed using Equation 1.

$$EVI = G \times \frac{(NIR - RED)}{(NIR + C_1 \times RED - C_2 \times BLUE + L)} \quad (1)$$

Decription:

G = 2.5 (gain factor)

C_1 = 6.0, C_2 =7.5 (coefficients for aerosol resistance)

L = 1.0 (canopy background adjustment)

NIR, RED, and BLUE = Surface reflectance values in the respective spectral bands

To detect burned areas and assess fire severity, the Normalized Burn Ratio (NBR) was used. NBR is derived from the difference between near-infrared (NIR) and shortwave infrared (SWIR) reflectance [14]. Vegetated areas typically exhibit high NIR and low SWIR reflectance, while post-fire areas show the opposite pattern. NBR values range from -1 to 1, with lower values indicating greater burn severity. The index is calculated using Equation 2.

$$NBR = \frac{(NIR - SWIR)}{(NIR + SWIR)} \quad (2)$$

Burned and unburned areas were identified using the Normalized Burn Ratio (NBR). The analysis involved two temporal stages: pre-fire (NBR_{pre}) and post-fire (NBR_{post}). A burned area is indicated by a significant decrease in NBR values after the fire event. The change in NBR (*dNBR*) computed according to Equation 3.

$$dNBR = NBR_{pre} - NBR_{post} \quad (3)$$

Description:

dNBR = change in NBR value

NBRpre = NBR value before fire

NBRpost = NBR value after fire

Burned areas were then classified using a threshold model. Thresholds were determined using the mean (μ) and standard deviation (σ) of sample pixels from known burned areas in the NBR imagery, following the approach by Fraser and Cihlar [21] (Equation 4).

$$\alpha = (\mu + \sigma) \text{ and } \beta = (\mu - \sigma) \quad (4)$$

Description:

α : Threshold of burnt area based on NBRpost

β : Threshold of burnt area based on dNBR

A pixel is classified as burned if it meets condition specified in Equation 5.

$$BA = dNBR \geq \alpha, \text{and } NBR_{post} \leq \beta \quad (5)$$

where BA indicates the burned area.

Temporal Dynamics of Vegetation Patterns in Fire-Affected Areas

The study approached spatial EVI time-series data as multi-dimensional signals and analyzed them with signal processing methods. To distinguish various temporal patterns, we performed K-means clustering with Euclidean distance in the EVI feature space, treating each EVI image as a separate dimension. This clustering grouped regions with similar EVI trends across time, enabling us to discern distinct characteristics of fire-affected areas. A similar approach was used by Setiawan et al. [22] for land use classification based on seasonal vegetation changes.

$$T^{(i)}(f_k) + \varepsilon^{(i)} = X_k^{(i)} \quad (6)$$

where *X* is a cluster, which describes the matrix of Euclidean distances between objects by hierarchical clustering algorithm, *f* is a signal, $\varepsilon^{(i)}$ is a centered Gaussian white noise of variance σ^2 independent of *k* and *i* and where $T^{(i)}$ is a slight deformation transforming a given function *g* as shown in Equation 7.

$$d^{(i)} g\left(\frac{x - b^{(i)}}{a^{(i)}}\right) = T^{(i)}(g(x)) \quad (7)$$

where $b^{(i)}$ is around 0, and $a^{(i)}$, $d^{(i)}$ around 1.

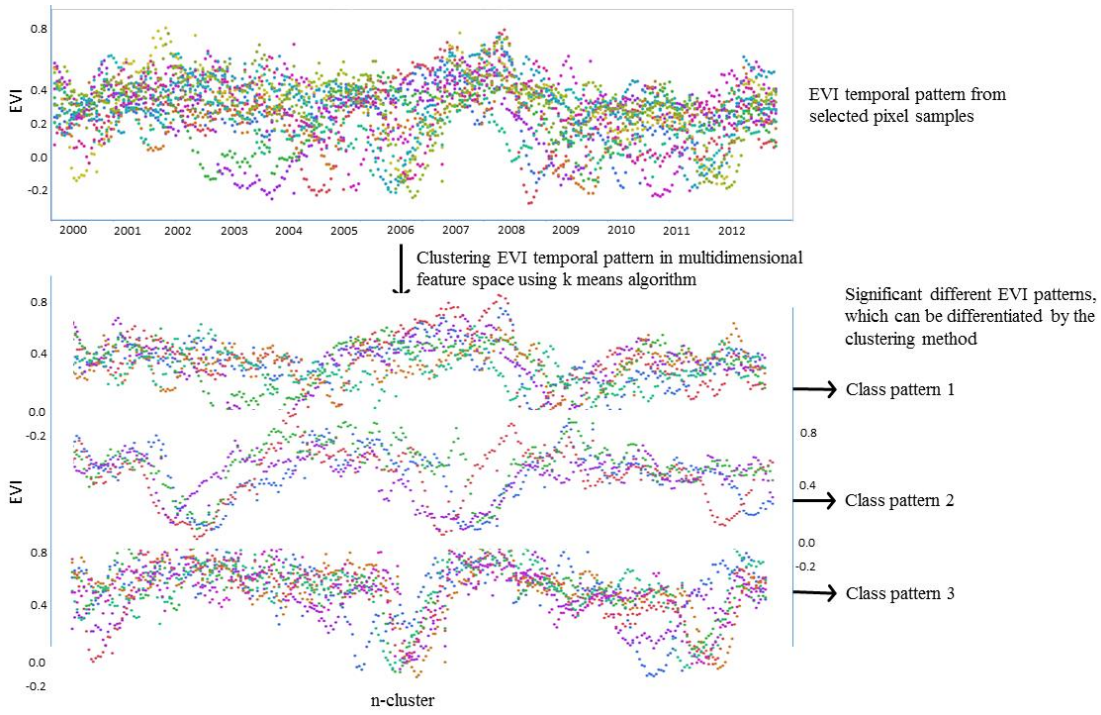

Figure 2. Clustering the EVI temporal pattern in multidimensional feature space.

In this study, the complexity and enormous number of time-series EVI datasets may lead to the difficulty of obtaining the actual number of clusters. The separability analysis was applied to discriminate among high detailed significant patterns that were theoretically defined to portray the specific characteristics of each peat swamp area in the study site.

Temporal Dynamics of Vegetation Patterns in Fire-Affected Areas

Vegetation surveys were conducted by recording the composition and structure of plant communities across different growth stages, including understorey, seedlings, saplings, poles, and trees within designated observation plots. For understorey, seedlings, and saplings, data collected consisted of species identity and

abundance, while for poles and trees, additional parameters such as species, population size, diameter, and height were measured.

Sampling was carried out in burnt areas using purposive sampling, with each main plot measuring 20 × 20 m. A nested sampling design was then applied, in which the main plot was subdivided into different subplot sizes: 20 × 20 m for trees, 10 × 10 m for poles, 5 × 5 m for saplings, and 2 × 2 m for seedlings and understorey vegetation [23]. At each location, vegetation was observed at varying fire frequencies: once, twice, three times, and four times. In total, 7 plots were established in once-burnt areas, 3 in twice-burnt areas, 4 in thrice-burnt areas, 2 in four-times-burnt areas, and 4 in unburned areas that served as controls. The number of observation points was determined based on the extent of each area and accessibility in the field.

To assess the vegetation structure at each sampling site, we measured several parameters of vegetation data such as: density, relative density, frequency, relative frequency, dominance, and relative dominance using Equations 8–13.

$$Density\ (D) = \frac{Total\ individuals\ of\ a\ species}{Total\ plot\ area} \quad (8)$$

$$Relative\ Density\ (RD) = \frac{Species\ density}{Total\ species\ density} \quad (9)$$

$$Frequency\ (F) = \frac{Number\ of\ plots\ occupied\ by\ a\ species}{Total\ number\ of\ observation\ plots} \quad (10)$$

$$Relative\ Frequency\ (RF) = \frac{Species\ frequency}{Total\ frequency\ of\ all\ species} \quad (11)$$

$$Dominance\ (Dc) = \frac{Total\ surface\ coverage\ of\ a\ species}{Total\ plot\ area} \quad (12)$$

$$Relative\ Dominance\ (RDc) = \frac{Dominance\ of\ a\ species}{Total\ dominance\ of\ all\ species} \quad (13)$$

Importance Value Index (IVI) for a species is is a sum of its relative density (RD), relative dominance (RDc) and relative frequency (RF) [24], which can be use to determine the influence given by a species to its community in an area.

The species diversity is important parameters in forest management [22]. Species diversity was determined using a Shannon-Wienner diversity index [24] (Equation 14).

$$Shannon\ Index\ H' = -\sum_{i=1}^{S} pi\ ln\ pi \quad (14)$$

where: *H'* = Plant Diversity, *Pi = Ni/N, Ni* = Number of individuals of each species, *N* = Total number of individuals from all species.

The Shannon Evenness Index (*E'*) is used to know the relative abundance of the different species of an ecosystem, with the equation 15.

$$Shannon\ Evennes\ indax\ (E') = \frac{H'}{ln\ S} \quad (15)$$

Species richness index does a relationship between the number of species and the number of individuals. Species richness was calculed using Margalef index [25] (Equation 16).

$$Margalef\ Index\ (R) = \frac{S-1}{ln\ N} \quad (16)$$

Sorensen Index was used to determinate the level of similariy species composition of the two communities being compered. Sorensen index is defined in Equation 17 [26].

$$Sorensen\ Index\ (SI) = \frac{2c}{S1+S2} \quad (17)$$

where: *S1* = Number of species for site 1, *S2* = Number of species for site 2, *c* = Number of common species between two sites.

Results and Discussion

Results

Landscape-Scale Peatland Ecosystem Structure and Ecological Heterogeneity

At the landscape scale, the eastern Sumatran peatlands exhibit substantial ecological heterogeneity influenced by peat depth, long-term hydrological processes, land-use history, and recurring anthropogenic disturbances. The multivariate clustering analysis of land-cover dynamics (2000–2020), peat depth, drainage

intensity, and fire occurrence resulted in the identification of 36 distinct peatland ecosystem classes (Figure 3). These classes represent a gradient ranging from relatively intact peat swamp forest ecosystems with higher biomass and stable hydrological conditions to severely degraded peatlands dominated by shrubs and plantation cover.

The mapped ecosystem classes form the baseline for characterizing spatial fire vulnerability and vegetation recovery patterns across the landscape.

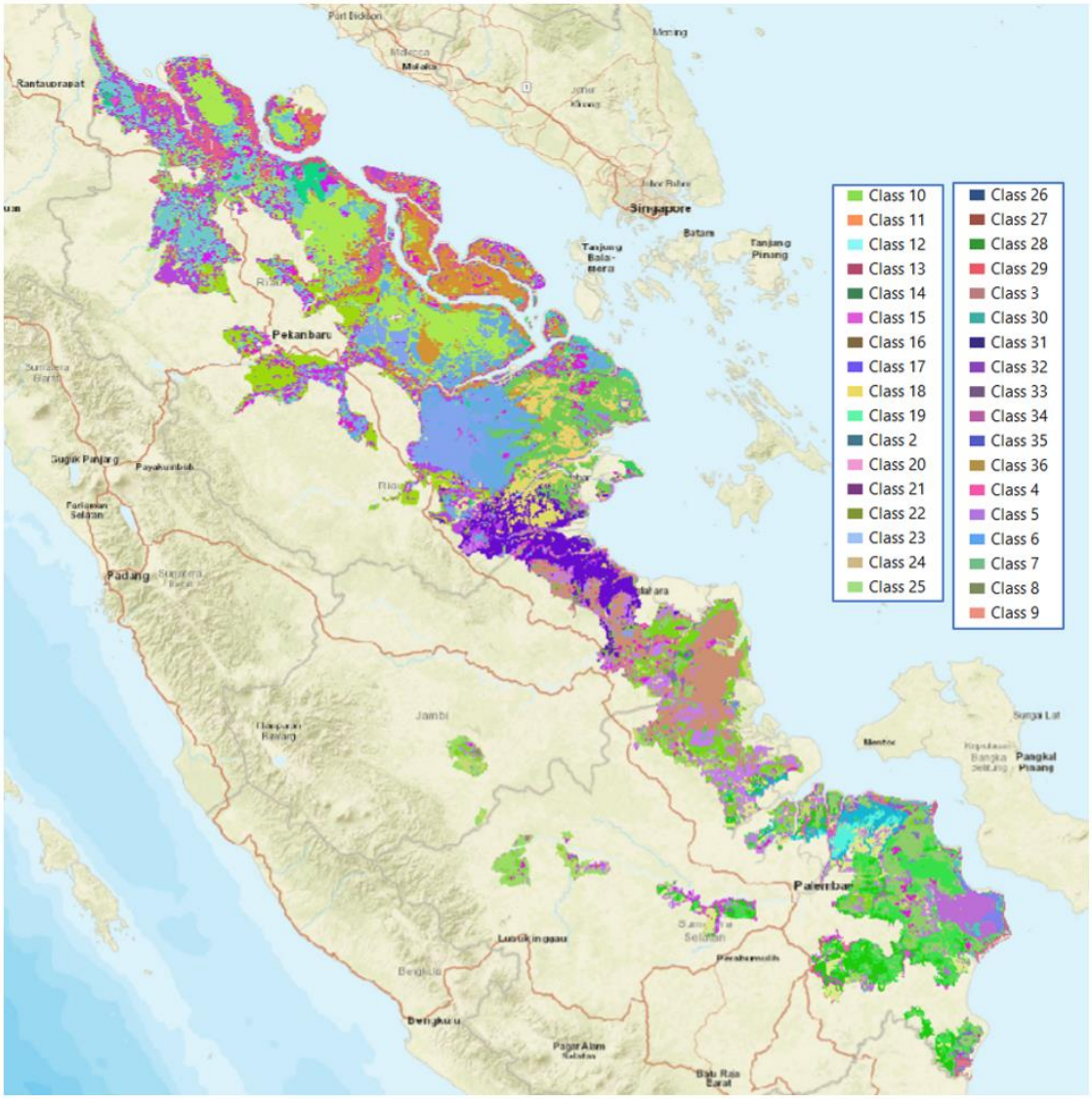

Figure 3. Classification of 36 peatland ecosystem types along the eastern coast of Sumatra, characterized by differences in temporal vegetation change (2000–2020), land cover composition, peat depth, and fire frequency.

Spatial Fire Vulnerability Across Ecosystem Classes

Hotspot distribution across the 36 peatland ecosystem classes during 2001–2020 demonstrates uneven spatial concentration of fire events (Figures 4–5). A small subset of classes — Class 5, 36, 13, 19, and 21 — contributed the majority of hotspot activity, with median hotspot densities reaching 20–106 hotspots ha^{-1}, and in several cases peaking above 300–500 hotspots ha^{-1}. These findings indicate that fire events are spatially clustered within specific ecosystem conditions. In contrast, intact peat swamp forest classes (1–3, 26, 29, and 34) consistently showed negligible fire occurrence during the same period.

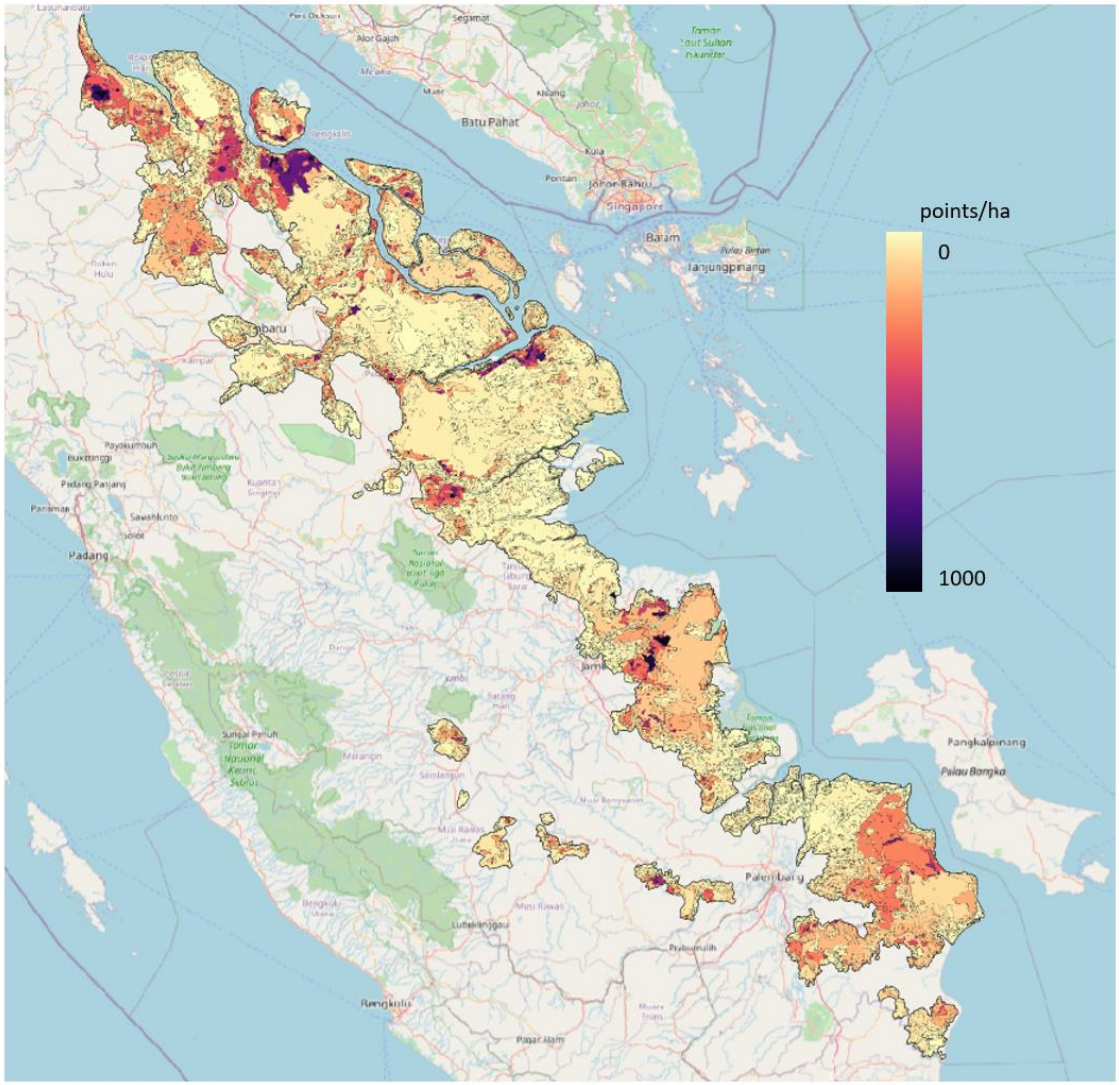

Figure 4. Distribution of fire hotspots per hectare within peatland ecosystems in eastern Sumatra.

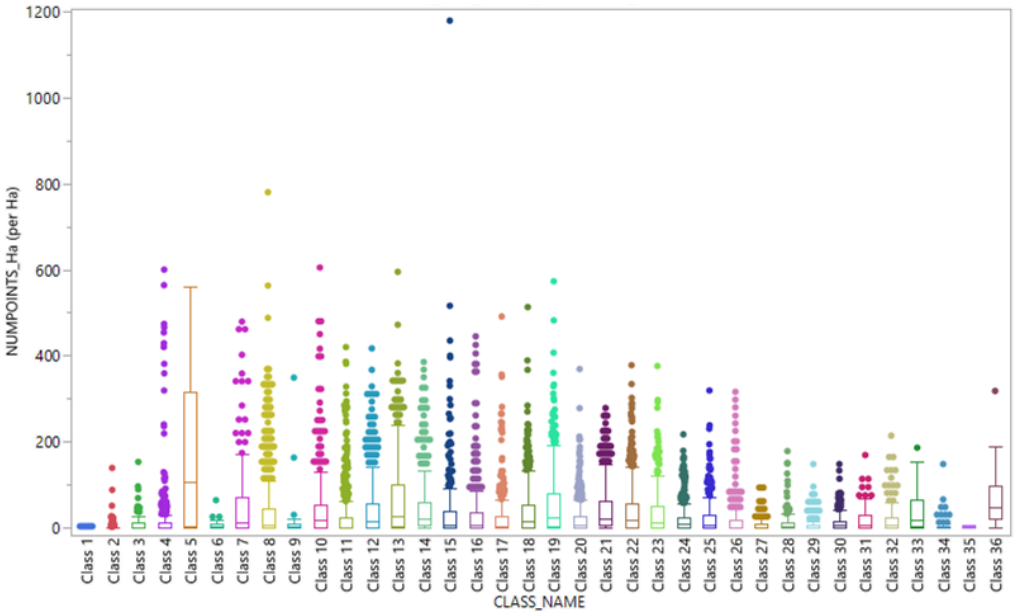

Figure 5. Variation in hotspot density among 36 ecosystem clusters during 2001–2020.

Burned Area Dynamics and Transformation of Fire Regimes

Burned-area mapping during significant fire years reveals major temporal shifts in burned land types (Figure 6). During the 1997 El Niño, burned areas were predominantly primary swamp forest, with a total of 13,931 ha recorded. In contrast, in 2015, burned areas were dominated by tree-crop plantations and industrial plantation forests, with a total burned area of 13,397 ha. This change represents a transition from earlier forest-based fire events toward fires occurring mainly in degraded and plantation-dominated peatlands.

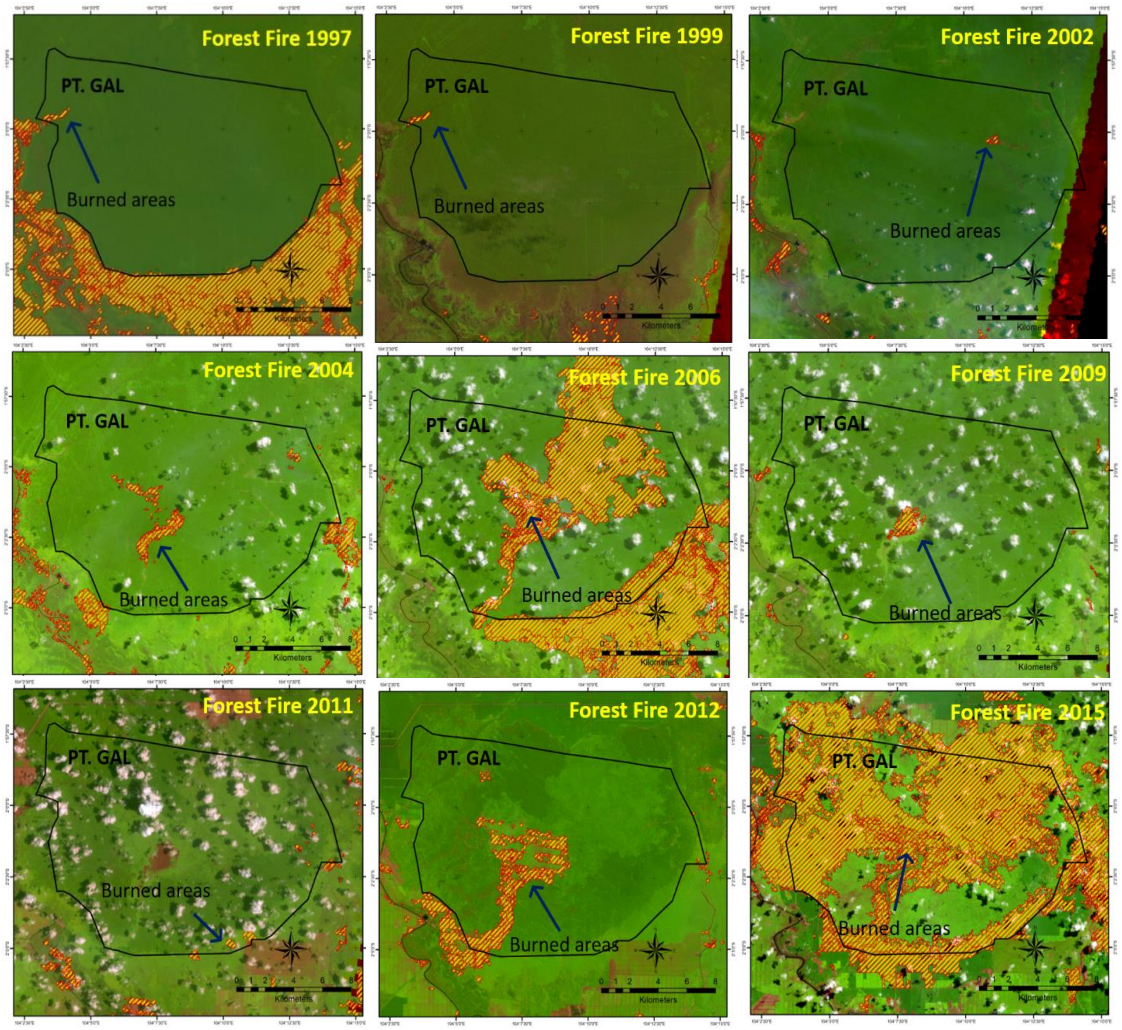

Figure 6. Burned-area maps representing major fire periods in the study area.

Fire Severity and Spectral Signatures

Fire-severity assessment using differenced Normalized Burn Ratio (dNBR) detected high-severity peat combustion in 2004 and 2015, indicated by dNBR >0.70. Pre-fire vegetation condition measured by EVI also exhibited a significant decline during the 2015 drought period, reaching 0.18, suggesting widespread canopy dryness. Table 1 shows four disturbance categories identified from the fire frequency analysis.

Table 1. Disturbance categories derived from the fire frequency analysis.

Fire frequency	Five years identified
Once-burned	2015
Twice-burned	2006, 2015
Three-times-burned	2006, 2012, 2015
Four-times-burned	1997, 2006, 2012, 2015

Temporal spectral profiles (Figure 8) show that repeatedly burned areas consistently maintain lower EVI/NBR values in post-fire recovery phases.

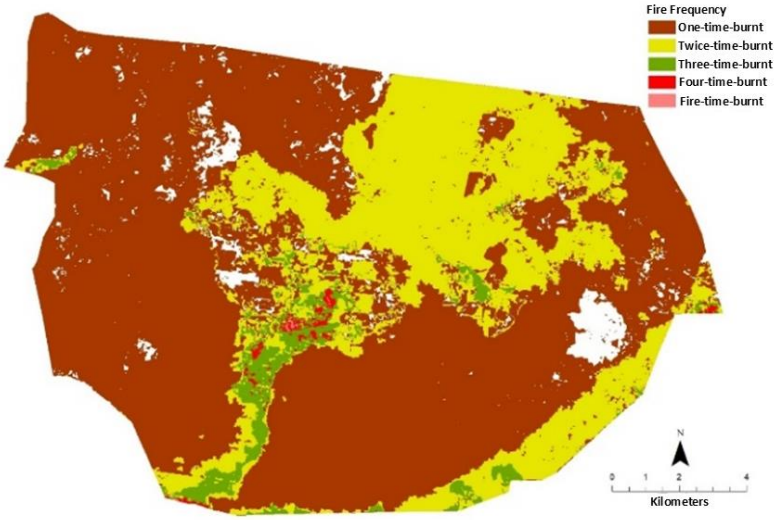

Figure 7. Fire frequency categories derived from multi-year Landsat burned-area history.

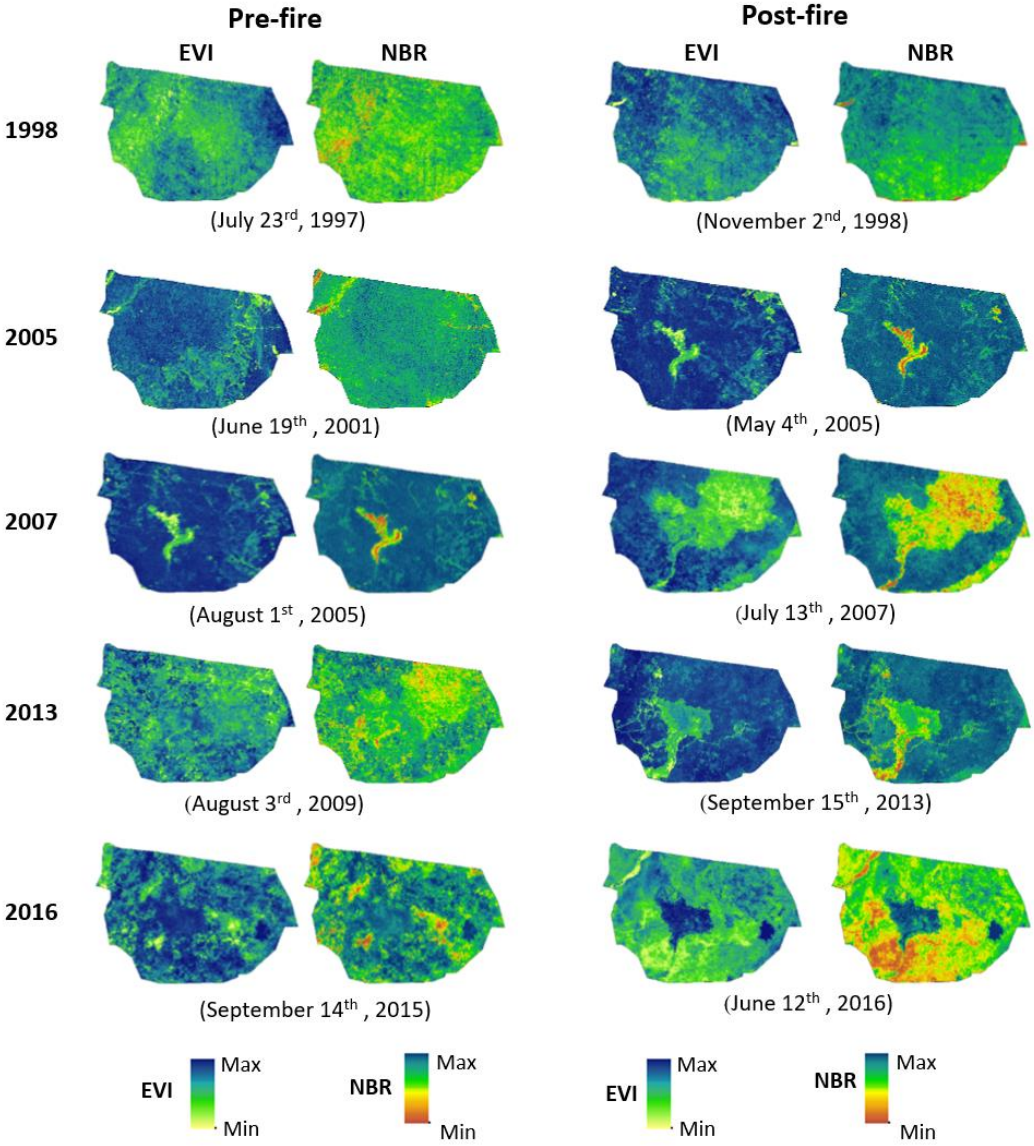

Figure 8. EVI and NBR time-series indicating vegetation condition under fire recurrence.

Species Composition and Dominance

Vegetation structure demonstrates strong differentiation across fire-frequency levels as shown in Table 1 and Figure 9. In once-burned areas, characteristic peat-swamp tree species were still present, including *Xylopia altissima*, *Macaranga pruinosa*, and *Cryptocarya griffithiana*, with IVI values of 94%, 84%, and 62%, respectively. In twice-burned areas, pole-size vegetation was dominated by *Macaranga pruinosa* and *Shorea parvifolia*. In three- and four-times-burned areas, no tree or pole species were recorded, indicating structural loss. Across higher fire-frequency categories, *Exbucklandia populnea* appeared consistently in the sapling strata. Understory communities were mainly dominated by *Asplenium longissimum* at 1–3 fire frequencies, shifting to *Athyrium esculentum* at 4-fire frequency locations.

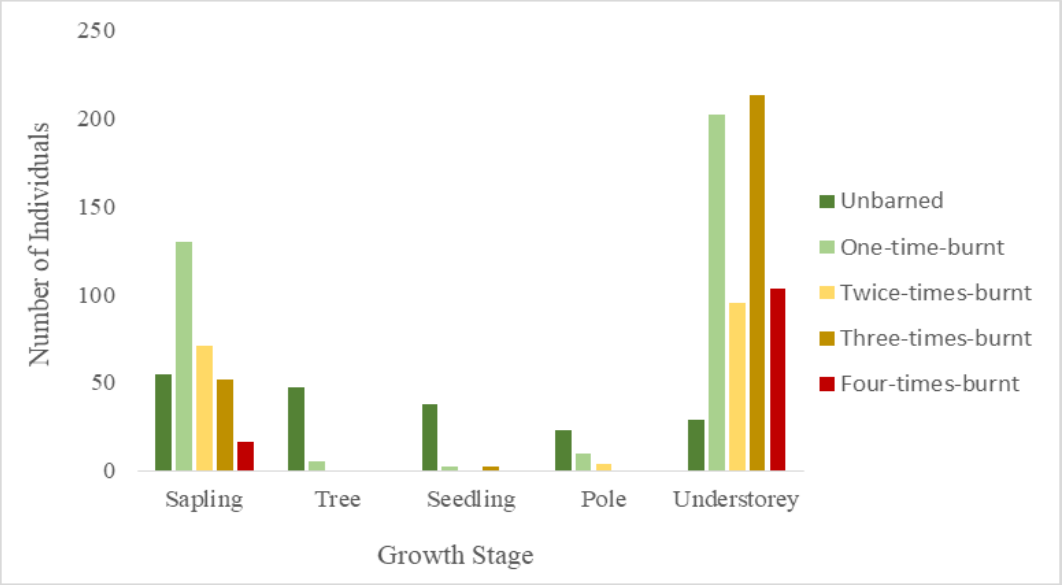

Figure 9. Vegetation structure under different fire frequencies.

Vegetation Diversity and Community Similarity

Diversity responses indicate that tree diversity was only present in one-time-burnt plots (H' = 1.33), while pole diversity declined to zero in two-burn plots. Sapling diversity remained low (H' = 0.50–0.90), and understory diversity increased at moderate fire frequency with H' values reaching up to 1.64 (Table 2). Meanwhile, community similarity analysis (Table 3) showed that sapling similarity across fire classes was mostly below 50%, whereas understory similarity was highest between three- and four-time burns (SI = 0.83).

Table 2. Plant diversity index in areas with different fire frequencies.

No	Growth Stage	Index	One-time-burnt	Twice-times-burnt	Three-times-burnt	Four-times-burnt
1	Tree	R	3.74	-	-	-
		H'	1.33	-	-	-
		E'	0.26	-	-	-
2	Pole	R	3.74	0.74	-	-
		H'	1.00	0.00	-	-
		E'	0.18	0.00	-	-
3	Sapling	R	10.74	4.74	1.74	1.74
		H'	0.69	0.90	0.69	0.50
		E'	0.01	0.19	0.05	0.46
4	Seedling	R	0.74	-	-	-
		H'	0.00	-	-	-
		E'	0.00	-	-	-
5	Understorey	R	3.74	5.74	6.74	4.74
		H'	1.10	1.26	1.64	1.44
		E'	0.25	0.20	0.15	0.19

Table 3. The similarity (SI) of sapling and understorey community in areas with different fire frequencies.

Sapling Community				
No	**Species Name**			
1	*Palaquium ridleyi*	*Melicope glabra*	*Alstonia pneumatophora*	*Macaranga pruinosa*
2	*Xylophia altissima*	*Nauclea orientalis*	*Exbucklandia populnea*	*Exbucklandia populnea*
3	*Macaranga pruinosa*	*Melaleuca cajuputi*		
4	*Cryptocarya crassinervia*	*Macaranga pruinosa*		
5	*Quasia borneensis*	*Leea indica*		
6	*Parkia speciosa*			
7	*Gluta renghas L.*			
8	*Gymnacranthera forbesii*			
9	*Dillenia ecxcelsa Gilg.*			
10	*Exbucklandia populnea*			
	1x	**2x**	**3x**	**4x**
1x	*	0.13	0.16	0.33
2x		*	0	0.28
3x			*	0.5
4x				*
Understorey Community				
No	**Species Name**			
1	*Asplenium longissimum*	*Eleusine indica*	*Imperata cylindrica*	*Eleusine indica*
2	*Athyrium esculentum*	*Asplenium longissimum*	*Eleusine indica*	*Asplenium longissimum*
3	*Lygodium flexuosum*	*Athyrium esculentum*	*Asplenium longissimum*	*Athyrium esculentum*
4	*Stenochlaena palustris*	*Stenochlaena palustris*	*Athyrium esculentum*	*Stenochlaena palustris*
5		*Alpinia galanga*	*Equisetum hyemale*	*Melastoma malabathricum*
6		*Melastoma malabathricum*	*Stenochlaena palustris*	
7			*Melastoma malabathricum*	
	1x	**2x**	**3x**	**4x**
1x	*	0.6	0.55	0.67
2x		*	0.62	0.73
3x			*	0.83
4x				*

1x = One-time-burnt, 2x = Twice-times-burnt, 3x = Three-times-burnt, 4x = Four-times-burnt.

Discussion

The presence of 36 peatland ecosystem classes identified through multivariate clustering demonstrates that peatland landscapes possess ecological zonation driven by peat depth, hydrological conditions, land-cover history, and disturbance intensity. This stratification is crucial because peatland fire behavior is not uniform across Sumatra; rather, it is determined by the interaction of hydrology, vegetation structure, and fuel moisture — variables that differ significantly between ecosystem classes. Similar eco-regional approaches have been employed in high-impact peatland studies to demonstrate that ecological zonation strongly influences the spatial distribution of vulnerability and recovery potential [27,28]. The presence of relatively intact forest classes embedded within a matrix of disturbed peatlands further highlights the fragmentation of peat ecosystems, with implications for fire propagation, hydrological connectivity, and the capacity for post-fire regeneration.

The identification of 36 ecosystem types thus provides the ecological framework necessary to interpret fire patterns and recovery trajectories at finer spatial scales. Without this landscape-based baseline, plot-level patterns would appear isolated; the hierarchical approach adopted here allows local ecological outcomes to be understood as emergent properties of broader landscape processes.

Fire hotspot analysis reveals that fire occurrence is not random but concentrated in a small number of degraded ecosystem classes (5, 36, 13, 19, and 21). These fire-prone classes share several ecological characteristics, including intensive drainage, conversion to plantations or open shrubland, high peat oxidation, and a prolonged history of recurrent burning. This pattern is consistent with the global peat–fire feedback theory, which suggests that hydrological degradation reduces peat moisture, increases fuel availability, and heightens the likelihood of surface-to-deep peat combustion [29]. In contrast, relatively intact peat swamp forest classes (e.g., Classes 1–3, 26, 29, 34) exhibit consistently low hotspot occurrence, reflecting more stable hydrological function, closed-canopy conditions, and limited anthropogenic ignition.

These findings affirm that landscape-level hydrological integrity remains the strongest natural defense against peatland fires [30,31]. Thus, fire in Sumatra's peatlands does not occur randomly but follows a spatial logic imposed by ecological condition, human influence, and long-term degradation patterns. Recognizing these spatially explicit vulnerability profiles is critical for designing targeted restoration and fire-prevention policies at the landscape scale.

Burned-area mapping during significant fire years indicates a substantial transformation in the land-cover categories affected by fire (Figure 6). During the 1997 El Niño event — one of the most severe droughts of the late twentieth century — burned areas were predominantly composed of primary peat swamp forests. This suggests profound hydrological stress even in relatively intact ecosystems under extreme climatic conditions and aligns with the extensive peat combustion reported elsewhere in Indonesia during the same period [32]. In contrast, the 2015 fire event presents a markedly different scenario: burned areas were primarily composed of tree-crop plantations, industrial plantation forests, and degraded peatlands. This shift reflects a landscape that has experienced decades of ecological simplification. The conversion to plantations, construction of drainage canals, and recurrent burning have transformed formerly resilient peat ecosystems into fire-prone landscapes. Such transitions — from forest-dominated to commodity-driven peatland mosaics with high fire susceptibility — have been documented at the regional scale by [33].

Quantitatively, the largest burned areas were recorded in 1997 (13,931 ha) and 2015 (13,397 ha). In 1997, primary forests (swamp, dryland, and mangrove) constituted the greatest share of burned area, whereas in 2015, the largest burned areas were in tree crop plantation (>16,773 ha) and plantation forest (>19,275 ha). These temporal changes illustrate an important ecological principle: as peatlands degrade, their fire regimes shift from predominantly climate-driven, episodic events (e.g., 1997) toward human-mediated, recurrent fires (e.g., 2015 onward). Present-day fire dynamics therefore need to be interpreted as outcomes of long-term landscape transformation rather than short-term climatic variability alone.

Fire-severity maps derived from the differenced Normalized Burn Ratio (dNBR) emphasize notable high-severity burns, particularly in 2004 and 2015, where dNBR values exceeded 0.70, signifying deep peat combustion and nearly complete canopy removal. These high-severity zones closely correspond with areas experiencing extended hydrological degradation, frequent fires, and extensive drainage, reinforcing the notion that severely degraded peatlands are more susceptible to intense fires. This trend aligns with remote sensing studies indicating that deep-burning peat fires produce distinct NBR signatures associated with peat-layer consumption, soil carbon loss, and long-term vegetation mortality [34]. Spectral indices, especially EVI and NBR, further indicate that the condition of vegetation prior to major fires is significantly influenced by large-scale climatic and hydrological stress. In 2015, pre-fire EVI values fell to 0.18, reflecting severe canopy desiccation due to El Niño–induced moisture deficits. The widespread decline across vast areas mirrors broad-scale physiological stress similar to that reported by [30].

Post-fire reductions in EVI and NBR are significant across all fire years, with NBR providing the clearest distinction between burned and unburned areas due to its sensitivity to NIR–SWIR differences, which respond to charcoal, ash, and exposed soil [14]. The fire-frequency gradient established in this study — once-burned, twice-burned, three-times-burned, and four-times-burned — is essential for comprehending how repeated burning induces ecological regime shifts at the site level. Repeated fire exposure results in a progressive collapse of vegetation structure. Once-burned plots still support vegetation across all growth stages, from understory and seedlings to saplings, poles, and trees. Twice-burned plots retain poles, saplings, and understory, but trees and seedlings are scarce or absent. In three-times-burned plots, only saplings, seedlings, and understory remain, while poles and trees are no longer present. Four-times-burned plots are reduced to saplings and understory only.

These structural changes align with the hypothesis that increasing fire frequency alters peat hydrology [35] and soil chemical properties [36] in ways that diminish the ability of tree species to persist. Extreme hydrological conditions and low-nutrient, acidic soils in peat swamp forests already pose limitations for many tree species [37]; repeated fires further exacerbate these constraints, driving stands toward open, low-stature vegetation. Time-series EVI and NBR profiles stratified by fire frequency demonstrate that all burned areas exhibit lower spectral index values in post-fire periods compared to pre-fire conditions. Unburned areas maintain higher index values, whereas repeatedly burned areas show persistently suppressed, fluctuating values, indicating slowed or arrested vegetation recovery. This dynamic reflects secondary succession processes repeatedly interrupted by fire. Severe peatland fires are known to require decades for meaningful recovery [38,39], and under repeated disturbance, the system may never return to pre-fire forest conditions [40].

The composition and dominance of plant species along the fire-frequency gradient reinforce this successional shift. Characteristic peat swamp species dominate once-burned areas but are progressively absent toward high-frequency fire plots. The persistence of Macaranga pruinosa across disturbance gradients aligns with its colonization capacity in degraded peatlands [41]. Understory vegetation becomes increasingly dominated by disturbance-tolerant ferns (*Asplenium longissimum*, *Athyrium esculentum*). These IVI patterns highlight a transition from tree-dominated communities to shrub–fern assemblages in areas subjected to frequent burning, driven by species with traits that confer high fire tolerance such as rhizomatous growth, rapid vegetative regeneration, and tolerance to nutrient-poor peat soils.

Vegetation diversity results further support this trajectory. Higher fire frequencies are associated with decreased species richness and increased community homogenization. Tree and pole diversity collapse after repeated fires [42], whereas understory diversity increases as early successional species proliferate. This suggests that high fire frequency eliminates non-fire-resistant species and favors species with rapid dispersal or vegetative regrowth capacity — consistent with previous research reporting dominance of herbaceous pioneers within 1–7 years after fire [43,44]. Sapling community similarity decreases with increased fire frequency, reflecting strong species turnover. However, understory communities converge toward similar composition across high burn frequencies (SI up to 83%), indicating a shift toward simplified assemblages and reduced beta diversity.

Overall synthesis of results across spatial scales demonstrates a consistent ecological pathway linking landscape degradation, fire regimes, and vegetation recovery. Degraded and repeatedly burned peatlands tend to transition toward simplified vegetation states with slow or arrested recovery. Landscape hydrological condition emerges as a foundational determinant of fire persistence and vegetation regrowth. Peatland recovery cannot be understood solely from plot-level monitoring; it is shaped by interactions between landscape hydrology, disturbance history, fire frequency, and vegetation feedbacks. These findings emphasize that restoration strategies must address hydrological degradation at the landscape scale, ensure sustained fire prevention, and support assisted regeneration where natural recovery stalls.

Conclusions

This study reveals that patterns of vegetation recovery in fire-affected peatlands of eastern Sumatra are strongly structured by landscape heterogeneity, fire regime characteristics, and cumulative disturbance intensity. At the landscape scale, 36 peatland ecosystem classes were identified, and only a small subset—characterised by severe hydrological degradation and land-cover conversion—concentrated the majority of fire occurrences. Burned-area mapping showed a clear long-term shift from climate-driven fires affecting primary peat swamp forests in 1997 toward recurrent human-mediated fires dominated by plantation landscapes in 2015.

Fire severity (dNBR) and spectral indices (EVI, NBR) demonstrated that the most degraded ecosystem classes experienced the highest levels of canopy loss and peat combustion, with widespread spectral instability even in non-fire years. At the plot scale, fire frequency emerged as the strongest predictor of ecological response: once-burned areas retained multi-layer forest structure, whereas three- and four-times-burned areas showed a near-complete collapse of tree and pole strata, a shift to shrub–fern dominance, reduced species richness, and increasing community homogenisation.

Overall, the findings indicate that repeated fire drives a transition from peat swamp forest to simplified, disturbance-tolerant vegetation assemblages with limited natural recovery capacity. This multi-scale evidence highlights that restoring fire-affected peatlands will require interventions that address both landscape-level hydrological degradation and site-level ecological thresholds.

Author Contributions

YS: Conceptualization, Methodology, Formal Analysis, Visualization, Writing - Original Draft, Writing - Review & Editing, Project Administration; **KU**: Conceptualization, Methodology, Resources, Writing - Review & Editing; **SAH**: Methodology, Software, Formal Analysis, Data Curation, Visualization, Writing - Review & Editing; **MAH**: Formal Analysis, Validation, Writing - Review & Editing; **AJ**: Formal Analysis, Resources, Writing - Review & Editing; **EIP**: Writing - Review & Editing.

AI Writing Statement

The authors did not use any artificial intelligence assisted technologies in the writing process.

Conflicts of Interest

There are no conflicts to declare.

Acknowledgements

This research was supported by the RIIM LPDP Grant and the *Badan Riset dan Inovasi Nasional* (BRIN) under the *Program Riset dan Inovasi untuk Indonesia Maju* (RIIM) Batch 3, Contract No:4/IV/KS/05/2023 and No: 13955/IT3/PT.01.03/P/B/2023. We also extend our sincere appreciation to the Center for Environmental Research, International Research Institute for Environment and Climate Change (PPLH-LRI LPI, IPB), IPB University, as well as to our collaborating partners, including the Directorate of Forest Resources Inventory and Monitoring, Ministry of Forestry (MoF), Indonesia, and the Environmental Analysis and Geospatial Modelling Laboratory, Faculty of Forestry and Environment, IPB University, for their valuable support in field validation and data provision. We further acknowledge the contributions of our field teams, local stakeholders, and research collaborators, whose assistance was instrumental in the successful completion of this study.

References

1. Field, R.D.; van der Werf, G.R.; Shen, S.S.P. Human amplification of drought-induced biomass burning in Indonesia since 1960. *Nature Geoscience* **2009**, *2*, 185–188.
2. Andela, N.; Morton, D.C.; Giglio, L.; Paugam, R.; Chen, Y.; Hantson, S.; van der Werf, G.R.; Randerson, J.T. The Global Fire Atlas of individual fire size, duration, speed and direction. *Earth System Science Data* **2019**, *11*, 529–552, doi:10.5194/essd-11-529-2019.
3. Turetsky, M.R.; Benscoter, B.; Page, S.; Rein, G.; van der Werf, G.R.; Watts, A. Global vulnerability of peatlands to fire and carbon loss. *Nature Geoscience* **2015**, *8*, 11–14, doi:10.1038/ngeo2325.
4. Hooijer, A.; Page, S.; Canadell, J.G.; Silvius, M.; Kwadijk, J.; Wösten, H.; Jauhiainen, J. Current and future CO_2 emissions from drained peatlands in Southeast Asia. *Biogeosciences* **2010**, *7*, 1505–1514, doi:10.5194/bg-7-1505-2010.
5. Harrison, M.E.; Page, S.E. Regrading the peat swamp: Ecology, degradation, and conservation of Southeast Asian peatlands. *Biodiversity and Conservation* **2016**, *25*, 2133–2151.
6. Konecny, K.; Ballhorn, U.; Navratil, P.; Jubanski, J.; Page, S.E.; Tansey, K.; Hooijer, A.; Vernimmen, R.; Siegert, F. Variable carbon losses from recurrent fires in drained tropical peatlands. *Global Change Biology* **2016**, *22*, 1469–1480, doi:10.1111/gcb.13186.
7. Keeley, J.E. Fire intensity, fire severity and burn severity: a brief review and suggested usage. *International Journal of Wildland Fire* **2009**, *18*, 116–126, doi:10.1071/WF07049.
8. Dohong, A.; Aziz, A.A.; Dargusch, P. A review of the drivers of tropical peatland degradation in South-East Asia. *Land Use Policy* **2017**, *69*, 349–360, doi:10.1016/j.landusepol.2017.09.035.
9. Roy, D.P.; Boschetti, L.; Justice, C.O.; Ju, J. The Collection 5 MODIS burned area product—Global evaluation by comparison with the MODIS active fire product. *Remote Sensing of Environment* **2008**, *112*, 3690–3707, doi:10.1016/j.rse.2008.05.013.
10. Key, C.H.; Benson, N.C. Landscape Assessment: Ground measure of severity, the Composite Burn Index; and remote sensing of severity, the Normalized Burn Ratio. In *FIREMON: Fire Effects Monitoring and Inventory System*; Lutes, D.C., Keane, R.E., Caratti, J.F., Key, C.H., Benson, N.C., Sutherland, S., Gangi, L.J., Eds.; U.S. Department of Agriculture, Forest Service, Rocky Mountain Research Station: Fort Collins, Colorado, USA, 2006;
11. Tucker, C.J. Red and photographic infrared linear combinations for monitoring vegetation. *Remote Sensing of Environment* **1979**, *8*, 127–150, doi:10.1016/0034-4257(79)90013-0.

12. Huete, A.R.; Didan, K.; Miura, T.; Rodriguez, E.P.; Gao, X.; Ferreira, L.G. Overview of the radiometric and biophysical performance of the MODIS vegetation indices. *Remote Sensing of Environment* **2002**, *83*, 195–213, doi:10.1016/S0034-4257(02)00096-2.
13. Gao, X.; Huete, A.R.; Ni, W.; Miura, T. Optical–biophysical relationships of vegetation spectra without background contamination. *Remote Sensing of Environment* **2000**, *74*, 609–620, doi:10.1016/S0034-4257(00)00150-4.
14. Key, C.H.; Benson, N.C. Landscape assessment: Fire severity and dNBR. In *FIREMON: Fire Effects Monitoring and Inventory System*; Lutes, D.C., Keane, R.E., Caratti, J.F., Key, C.H., Benson, N.C., Sutherland, S., Gangi, L.J., Eds.; U.S. Department of Agriculture, Forest Service, Rocky Mountain Research Station: Fort Collins, Colorado, USA, 2006;
15. Verbesselt, J.; Hyndman, R.; Newnham, G.; Culvenor, D. Detecting trend and seasonal changes in satellite image time series. *Remote Sensing of Environment* **2010**, *114*, 106–115, doi:10.1016/j.rse.2009.08.014.
16. Setiawan, Y.; Kustiyo, K.; Hudjimartsu, S.A.; Purwanto, J.; Rovani, R.; Tosiani, A.; Usman, A.B.; Kartika, T.; Indriasari, N.; Prasetyo, L.B.; Margono, B.A. Evaluating Visible–Infrared Imaging Radiometer Suite Imagery for Developing Near-Real-Time Nationwide Vegetation Cover Monitoring in Indonesia. *Remote Sensing* **2024**, *16*, 1–19, doi:10.3390/rs16111958.
17. Setiawan, Y.; Prasetyo, L.B.; Pawitan, H.; Permatasari, P.A.; Suyamto, D.; Wijayanto, A.K. Identifying Areas Affected by Fires in Sumatra Based on Time Series of Remotely Sensed Fire Hotspots and Spatial Modeling. *Jurnal Pengelolaan Sumberdaya Alam dan Lingkungan* **2018**, *8*, 420–427, doi:10.29244/jpsl.8.3.420-427.
18. Vermote, E.F.; Roger, J.C.; Ray J.P. MODIS Surface Reflectance User's Guide Collection 6. 2015. Available online: https://modis-land.gsfc.nasa.gov/pdf/MOD09_UserGuide_v1.4.pdf (accessed on 15 July 2025).
19. Suyamto, D.; Prasetyo, L.; Setiawan, Y.; Wijaya, A; Kustiyo, K.; Kartika, T.; Effendi, H.; Permatasari, P. Measuring Similarity of Deforestation Patterns in Time and Space across Differences in Resolution. *Geomatics* **2021**, *1*, 464–495, doi:10.3390/geomatics1040027.
20. NASA FIRMS. Fire Information for Resource Management System (FIRMS) – MODIS & VIIRS Active Fire Data. Available online: https://firms.modaps.eosdis.nasa.gov/ (accessed on 20 July 2025).
21. Fraser, R.H.; Cihlar, J. Hotspot and NDVI differencing synergy (HANDS): a new technique for burned area mapping over boreal forest. *Remote Sensing of Environment* **2000**, *74*, 362–376.
22. Setiawan, Y.; Yoshino, K.; Philpot, W.D. Characterizing temporal vegetation dynamics of land use in regional scale of Java Island, Indonesia. *Journal of Land Use Science* **2013**, *8*, 1–30, doi:10.1080/1747423X.2011.605178.
23. Silviana, S.H.; Saharjo, B.H.; Sutikno, S. Effect of wildfires on tropical peatland vegetation in Meranti Islands district, Riau province, Indonesia. *Biodiversitas* **2019**, *20*, 3056–3062.
24. Prayoto; Firdaus, R.; Nakagoshi, N. Tree species diversity and structural composition of tropical peat swamp forest : a study in Riau, Indonesia. *Hikobia* **2018**, 17, 261–271.
25. Soerianegara, I.; Indrawan, A. *Ekologi Hutan Indonesia*. IPB University: Bogor, ID, 1978;
26. Supriatna, J. Biodiversity Indexes: Value and Evaluation Purposes. In Proceedings of the 4th International Workshop on UI GreenMetric World University Rankings (IWGM 2018), Semarang, ID, 8–10 April 2018.
27. Page, S.E.; Rieley, J.O.; Banks, C.J. Global and regional importance of the tropical peatland carbon pool. *Global Change Biology* **2011**, *17*, 798–818, doi:10.1111/j.1365-2486.2010.02279.x.
28. Warren, M.; Hergoualc'h, K.; Murdiyarso, D. Carbon consequences of fire in tropical peatlands. *Global Change Biology* **2017**, *23*, 478–489.
29. Turetsky, M.R.; Benscoter, B.; Page, S.; Rein, G.; van der Werf, G.R.; Watts, A. Global vulnerability of peatlands to fire and carbon loss. *Nature Geoscience* **2015**, *8*, 11–14, doi:10.1038/ngeo2325.
30. Hoscilo, A.; Page, S.E.; Tansey, K.J.; Rieley, J.O. Effect of repeated fires on land-cover change on peatland in southern Central Kalimantan, Indonesia, from 1973 to 2005. *International Journal of Wildland Fire* **2011**, *20*, 578–588, doi:10.1071/WF10029.

31. Konecny, K.; Ballhorn, U.; Navratil, P.; Jubanski, J.; Page, S.E.; Tansey, K.; Hooijer, A.; Vernimmen, R.; Siegert, F. Variable carbon losses from recurrent fires in drained tropical peatlands. *Environmental Research Letters* **2016**, *11*, 1469–1480, doi:10.1111/gcb.13186.
32. Page, S.E.; Siegert, F.; Rieley, J.O.; Boehm, H.-D.V.; Jaya, A.; Limin, S. The amount of carbon released from peat and forest fires in Indonesia during 1997. *Nature* **2002**, *420*, 61–65, doi:10.1038/nature01131.
33. Miettinen, J.; Shi, C.; Liew, S.C.; Kwoh, L.K. Land cover distribution in the peatlands of Peninsular Malaysia, Sumatra and Borneo in 2015 with changes since 1990. *Global Ecology and Conservation* **2017**, *6*, 67–78, doi:10.1016/j.gecco.2016.02.004.
34. Ballhorn, U.; Siegert, F.; Mason, M.; Limin, S. Derivation of burn scar depths and estimation of carbon emissions with LIDAR in Indonesian peatlands. *Proceedings of the National Academy of Sciences* **2009**, *106*, 21213–21218, doi:10.1073/pnas.0906457106.
35. Brown, C.; Bousfield, C.; Waddington, J.M. Vegetation impact on peatland hydrology after wildfire. *Hydrological Processes* **2015**, *29*, 442–456.
36. Sazawa, K.; Wakimoto, T.; Fukushima, M.; Yustiawati, Y.; Syawal, M.S.; Hata, N.; Taguchi, S.; Tanaka, S.; Tanaka, D.; Kuramitz, H. Impact of Peat Fire on the Soil and Export of Dissolved Carbon in Tropical Peat Soil, Central Kalimantan, Indonesia. *ACS Earth and Space Chemistry* **2018**, *2*, 640–752, doi:10.1021/acsearthspacechem.8b00018.
37. Posa, M.R.C.; Wijedasa, L.S.; Corlett, R.T. Biodiversity and conservation of tropical peat swamp forests. *Biodiversity and Conservation* **2011**, *20*, 2965–2988, doi:10.1525/bio.2011.61.1.10.
38. Dharmawan, I.W.E. Forest recovery time in tropical peatlands after fire. *Forest Science and Technology* **2012**, *8*, 103–108.
39. Guêné-Nanchen, M.; LeBlanc, M.C.; Rochefort, L. Post-fire peatland vegetation recovery: a case study in open rich fens of the Canadian boreal forest. *Botany* **2022**, *100*, 435–447, doi:10.1139/cjb-2021-0194.
40. FAO. Peatlands – Guidance for Climate Change Mitigation through Conservation, Rehabilitation and Sustainable Use, 2nd ed.; Joosten, H.; Tapio-Biström, M.-L., Tol, S., Eds.; FAO and Wetlands International: Rome, Italy, 2012; ISBN 978-92-5-107302-5.
41. Yule, C.M. Loss of biodiversity and ecosystem functioning in peat swamp forests. *Biodiversity and Conservation* **2010**, *19*, 393–409, doi:10.1007/s10531-008-9510-5.
42. Balch, J.K.; Massad, T.J.; Brando, P.M.; Nepstad, D.C.; Curran, L.M. Effects of high-frequency understorey fires on woody plant regeneration in southeastern Amazonian forests. *Philosphical Transactions of The Royal Society B* **2013**, *368*, 20120157, doi:10.1098/rstb.2012.0157.
43. Gandiwa, E. Effects of repeated burning on woody vegetation structure and composition in a semi-arid southern African savanna. *International Journal of Environmental Science* **2011**, *2*, 458–471.
44. Malkisnon, D.; Wittenberg, L.; Beeri, O.; Barzilai, R. Effects of Repeated Fires on the Structure, Composition, and Dynamics of Mediterranean Maquis: Short- and Long-Term Perspectives. *Ecosystems* **2011**, *14*, 478–488, doi:10.1007/s10021-011-9424-z.